INSTITUTE OF PHYSICS PUBLISHING EUROPEAN JOURNAL OF PHYSICS

Eur. J. Phys. **26** (2005) 205–215 doi:10.1088/0143-0807/26/1/021

Detecting chaos from a time series

Stane Kodba, Matjaž Perc and Marko Marhl

Department of Physics, Faculty of Education, University of Maribor, Koroška cesta 160, SI-2000 Maribor, Slovenia

E-mail: marko.marhl@uni-mb.si

Received 16 September 2004, in final form 7 November 2004
Published 29 December 2004
Online at stacks.iop.org/EJP/26/205

Abstract

The chaotic behaviour of a driven resonant circuit is studied directly from the experimental data. We use basic nonlinear time series analysis methods that are appropriate for undergraduate courses. Mutual information and false nearest neighbours are explained in detail, and used to obtain the best possible attractor reconstruction. For the reconstructed attractor, a determinism test is performed and the largest Lyapunov exponent is calculated. We show that the largest Lyapunov exponent is positive, which is a strong indicator for the chaotic behaviour of the system. To help the reader reproduce our results and to facilitate further applications on other experimental systems, we provide user-friendly programs with graphical interface for each implemented method on our Web page.

1. Introduction

Four decades ago, the paradigm of chaos was introduced [1]. Since the discovery of chaos the interest in this field of research has risen rapidly. Several attempts have been made to integrate the chaos theory into the undergraduate curriculum [2–4]. Accordingly, simple experiments have been proposed [5–9] to demonstrate basic characteristics of chaotic behaviour, such as the irregularity of motion, unpredictability and sensitivity to initial conditions.

In many cases, the analysis of experimentally observed chaotic behaviour is for simplicity reasons confined to computer simulations of appropriate mathematical models [10–12]. However, showing that a mathematical model exhibits chaotic behaviour is no proof that chaos is also present in the corresponding experimental system. To convincingly show that an experimental system behaves chaotically, chaos has to be identified directly from the experimental data. For this purpose, nonlinear time series analysis methods have to be applied [13–15].

In this paper, we use basic nonlinear time series analysis methods for confirming the chaotic behaviour of a very simple periodically driven resistor–inductor diode (RLC) circuit [16]. First, we use the delay coordinate embedding method for reconstructing the attractor

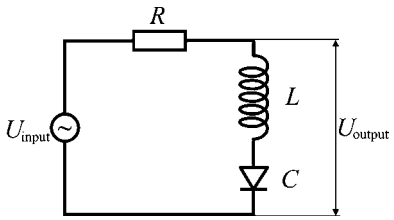

Figure 1. Schematic presentation of the experimental system.

of the system from the observed time series. For this purpose, we have to determine the proper embedding delay and embedding dimension. There exist two methods, developed in the framework of nonlinear time series analysis, that enable us to readily perform the desired tasks. The mutual information method [17] yields an estimate for the proper embedding delay, whereas the false nearest neighbour method [18] enables us to determine a proper embedding dimension. Second, we perform a simple determinism test [19]. The latter is of crucial importance, since it enables us to distinguish between deterministic chaos and irregular random behaviour, which often resembles chaos, but originates from a stochastic system. Finally, to determine the presence of deterministic chaos in the driven RLC circuit, we calculate the largest Lyapunov exponent. We show that the largest Lyapunov exponent is positive, which is a strong indicator for the presence of chaos in the examined system.

To help the reader reproduce our results, and to facilitate further applications on other experimental systems, we provide user-friendly programs with a graphical interface for each implemented method. The whole program package, including step-by-step usage guidance, can be downloaded from our Web page [20].

2. Experiment

We study a simple periodically driven RLC circuit [16] (see figure 1). The circuit elements have values $R = 200\ \Omega$, $L = 0.1$ mH, while the diode is a classical 1N4007 silicon rectifier with a typical junction capacitance of approximately 30 pF. The output (U_{output}) voltage has been measured with a LeCroy digital oscilloscope with a sampling rate of 500 measurements per second.

In dependence on the amplitude of the input sinusoidal voltage ($U_{\text{input},0}$), the circuit exhibits various regular and complex oscillations. If $U_{\text{input},0} \approx \pm 0.5$ V, the system oscillates regularly with a resonant frequency of 2.2 Hz. The corresponding two-dimensional phase space projection U_{input} versus U_{output} is shown in figure 2(a). When $U_{\text{input},0}$ is increased to approximately ± 1.5 V, we obtain a two-folded limit cycle (figure 2(b)). At even higher values of $U_{\text{input},0}$, the limit cycle undergoes further period doublings (see figure 2(c)), until eventually the behaviour becomes chaotic as shown in figure 2(d).

Although results presented in figure 2 indicate a typical period doubling route to chaos, a more detailed and careful approach is required to truly confirm the presence of deterministic chaos in the examined system. For this purpose, we collect 25 000 data points of the output voltage presented in figure 2(d), and apply nonlinear time series analysis methods in order to confirm the chaotic behaviour of the system.

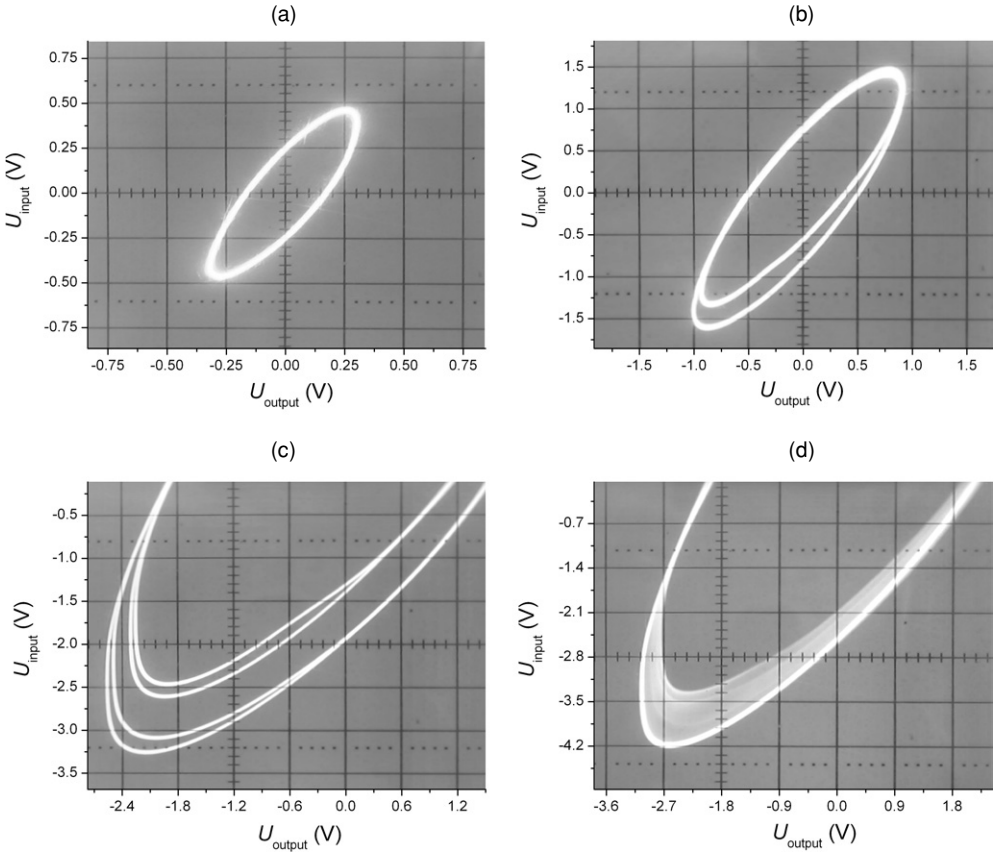

Figure 2. System behaviour in dependence on the amplitude of the input sinusoidal voltage ($U_{\text{input},0}$). The experimental results are shown as 2D phase space projections of the input versus output voltage. (a) Regular behaviour in the form of a simple limit cycle at $U_{\text{input},0} = \pm 0.5$ V. (b) Regular behaviour in the form of a two-folded limit cycle at $U_{\text{input},0} = \pm 1.5$ V. (c) Regular behaviour in the form of a four-folded limit cycle at $U_{\text{input},0} = \pm 3.0$ V. (d) Chaotic behaviour at $U_{\text{input},0} = \pm 4.0$ V.

3. Time series analysis

3.1. Reconstruction of the attractor

At first, the reconstruction of the attractor in an m-dimensional phase space appears to be a rather complicated task, since we only have the time series of a single system variable. In our experiment, we have measured the output voltage U_{output}. This gave us the time sequence of the form $\{x_0, x_1, x_2, \ldots, x_i, \ldots, x_n\}$, where x_i denotes the output voltage at time i. According to Takens [21] the reconstructed attractor of the original system is given by the vector sequence

$$\mathbf{p}(i) = (x_i, x_{i+\tau}, x_{i+2\tau}, \ldots, x_{i+(m-1)\tau}), \tag{1}$$

where τ and m are the embedding delay and the embedding dimension, respectively. The famous theorem by Takens [21] states that for a large enough m, this procedure, known as delay coordinate embedding, provides a one-to-one image of the original system. In other words, the attractor constructed according to equation (1) will have the same mathematical properties, such as the dimension, Lyapunov exponents, etc as the original system. Although the

concept of delay coordinate embedding may appear somewhat mystic, in particular the fact that one can reconstruct the whole phase space of a system from a single scalar measurement, there exists a rather intuitive explanation why the reconstruction can be made. According to Abarbanel [13], the key to understanding lies in the fact that all variables in a nonlinear process are generically connected, i.e. they influence one another. Thus, every subsequent point of a given measurement x_i is the result of an entangled combination of influences from all other system variables. Accordingly, $x_{i+\tau}$ may be viewed as a substitute second system variable, which carries information about the influences of all other variables during time τ. With the same reasoning one can introduce the 3rd ($x_{i+2\tau}$), 4th ($x_{i+3\tau}$), ..., mth ($x_{i+(m-1)\tau}$) substitute variable, and thus obtain the whole m-dimensional phase space where the substitute variables incorporate all influences of original system variables, provided m in equation (1) is large enough.

To reconstruct the attractor successfully by using equation (1), appropriate values for τ and m have to be determined. For estimation of τ, two criteria are important. First, τ has to be large enough so that the information we get from measuring the value of x at time $i + \tau$ is significantly different from the information we already have by knowing the value of x at time i. Only then will it be possible to gather enough information about all other system variables that influence the value of x to reconstruct the whole attractor. Second, τ should not be larger than the typical time in which the system loses memory of its initial state. This is particularly important for chaotic systems, which are intrinsically unpredictable and hence lose memory of the initial state as time progresses.

Following this reasoning, Fraser and Swinney [17] introduced the mutual information between x_i and $x_{i+\tau}$ as a suitable quantity for determining τ. The mutual information between x_i and $x_{i+\tau}$ quantifies the amount of information we have about the state $x_{i+\tau}$ presuming we know the state x_i. Given a time series of the form $\{x_0, x_1, x_2, \ldots, x_i, \ldots, x_n\}$, one first has to find the minimum ($x_{\min}$) and the maximum ($x_{\max}$) of the sequence. The absolute value of their difference $|x_{\max} - x_{\min}|$ then has to be partitioned into j equally sized intervals, where j is a large enough integer number. Finally, one calculates the expression

$$I(\tau) = -\sum_{h=1}^{j}\sum_{k=1}^{j} P_{h,k}(\tau) \ln \frac{P_{h,k}(\tau)}{P_h P_k}, \tag{2}$$

where P_h and P_k denote the probabilities that the variable assumes a value inside the hth and kth bins, respectively, and $P_{h,k}(\tau)$ is the joint probability that x_i is in bin h and $x_{i+\tau}$ is in bin k. In order to better understand equation (2), let us consider a limit example. In the case of chaotic behaviour $I(\tau) \to 0$ as $\tau \to \infty$, since x_i and $x_{i+\tau}$ are then no longer correlated, and thus $P_{h,k}(\tau)$ factorizes to $P_h P_k$ yielding zero in equation (2). In general, we are interested in minima of $I(\tau)$. At the first minimum of $I(\tau)$ $x_{i+\tau}$ adds the largest amount of information to the information we already have by knowing x_i, without completely losing the correlation between them [17, 22]. Hence, the first minimum of $I(\tau)$ marks the optimal choice for the embedding delay.

For the oscillatory regime presented in figure 2(d), the first minimum of $I(\tau)$ is obtained at $\tau = 65$ time steps (see figure 3). This result can be easily reproduced with our program *mutual.exe*, which can be downloaded from our Web page [20]. The program has only two crucial parameters, which are the number of bins j (in our case 100) and the maximal embedding delay τ (in our case 500). All calculated results are displayed graphically. More precise usage instructions are given in the appendix and on the Web page.

To determine the proper embedding dimension m, we use the false nearest neighbour method [18]. The method relies on the assumption that an attractor of a deterministic system folds and unfolds smoothly with no sudden irregularities in its structure. Therefore, points

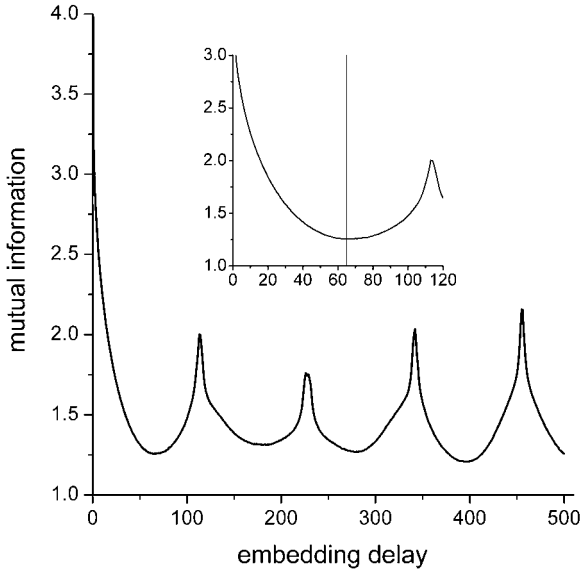

Figure 3. Determination of the proper embedding delay. The mutual information has the first minimum at $\tau = 65$.

that are close in the reconstructed embedding space have to stay sufficiently close also during forward iteration. If this criterion is met, then under some sufficiently short forward iteration the distance between two points $\mathbf{p}(i)$ and $\mathbf{p}(j)$ of the reconstructed attractor, which are initially only a small ε apart, cannot grow further as $R_{tr}\varepsilon$, where R_{tr} is a given constant (see below). However, if an ith point has a close neighbour that does not fulfil this criterion, then this ith point is marked as having a false nearest neighbour. We have to minimize the fraction of points having a false nearest neighbour by choosing a sufficiently large m. If m is too small, two points of the attractor may solely appear to be close, whereas under forward iteration they are mapped randomly due to projection effects. The random mapping occurs because the whole attractor is projected onto a hyperplane that has a smaller dimensionality than the actual phase space and so the distances between points become distorted.

In order to calculate the fraction of false nearest neighbours the following algorithm is used. Given a point $\mathbf{p}(i)$ in the m-dimensional embedding space, one first has to find a neighbour $\mathbf{p}(j)$, so that $\|\mathbf{p}(i) - \mathbf{p}(j)\| < \varepsilon$, where $\|\cdots\|$ is the square norm and ε is a small constant usually not larger than the standard deviation of data. We then calculate the normalized distance R_i between the $(m+1)$th embedding coordinate of points $\mathbf{p}(i)$ and $\mathbf{p}(j)$ according to the equation:

$$R_i = \frac{|x_{i+m\tau} - x_{j+m\tau}|}{\|\mathbf{p}(i) - \mathbf{p}(j)\|}. \tag{3}$$

If R_i is larger than a given threshold R_{tr}, then $\mathbf{p}(i)$ is marked as having a false nearest neighbour. Equation (3) has to be applied for the whole time series and for various $m = 1, 2, \ldots$ until the fraction of points for which $R_i > R_{tr}$ is negligible. According to Kennel *et al* [18], $R_{tr} = 10$ has proven to be a good choice for most data sets.

The results obtained with the false nearest neighbour method are presented in figure 4. It can be well observed that the fraction of false nearest neighbours (fnn) convincingly drops to zero for $m = 5$. This means that the studied periodically driven RLC circuit is a 5D system.

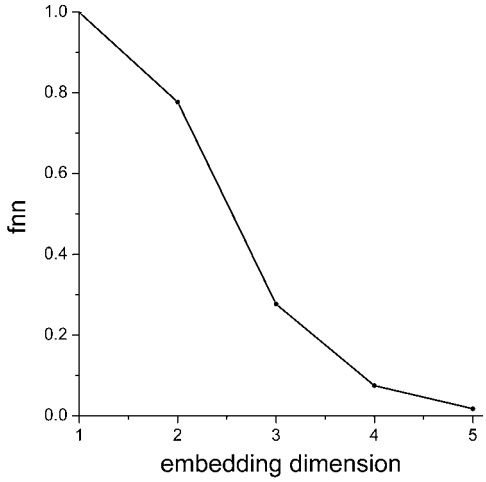

Figure 4. Determination of the minimal required embedding dimension. The fraction of false nearest neighbours (fnn) drops convincingly to zero at $m = 5$.

In other words, it would be justified to model the behaviour of the system with not less than five autonomous first-order ordinary differential equations.

This result can also be easily reproduced with our program *fnn.exe*, which can be downloaded from our Web page [20]. Parameter values that have to be provided are the minimal and the maximal embedding dimensions for which the fraction of false nearest neighbours is to be determined ($m_{\min} = 1, m_{\max} = 5$), the embedding delay ($\tau = 65$), the initial ε (0.05), and the factor for increasing the initial ε (1.41).

Having calculated the optimal embedding delay and embedding dimension, we are able to successfully reconstruct the attractor. For $m = 5$ and $\tau = 65$, the attractor obtained according to equation (1) is presented in figure 5. The correct reconstruction of the attractor is a key step towards establishing whether the experimentally observed behaviour originated from a deterministic chaotic system, since it enables us to perform the determinism test, and to calculate the largest Lyapunov exponent.

3.2. Determinism test

After reconstructing the attractor, we are able to perform the determinism test [19] to verify if the studied time series indeed originates from a deterministic system. The determinism test is of crucial importance since it enables us to distinguish between deterministic chaos and irregular random behaviour, which often resembles chaos.

By closely observing figure 5, it becomes evident that the measured data points are somewhat burdened with measurement error. The lines of the reconstructed phase space are not completely smooth. Thus, one may wonder if the irregular appearing attractor is truly a consequence of the underlying deterministic dynamics, or is it simply a consequence of random measurement error. To clarify this, a determinism test [19, 23, 24] has to be deployed.

If a system is deterministic, it can be described by a set of ordinary differential equations. The vector field at every point of the phase space is uniquely determined by the differential equations. Therefore, the determinism test introduced by Kaplan and Glass [19] enables us to construct the vector field of the system directly from the time series, and subsequently test if the reconstructed vector field assures uniqueness of solutions in the phase space. The

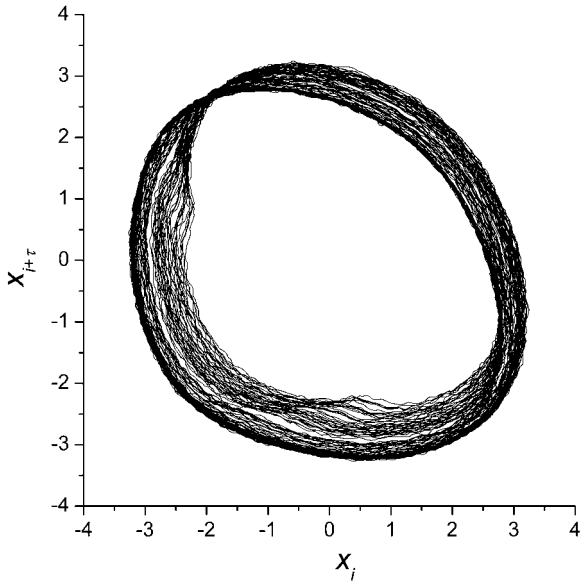

Figure 5. Reconstructed phase space obtained with the optimal embedding parameters: $\tau = 65$ and $m = 5$.

determinism test is based on a correct reconstruction of the attractor in the embedding space. The embedding space has to be coarse grained into equally sized boxes. To each box that is occupied by the trajectory a vector is assigned, which will finally be our approximation for the vector field. The vector pertaining to a particular box is obtained as follows. Each pass i of the trajectory through the kth box generates a *unit* vector $\mathbf{e}_i$ whose direction is determined by the phase space point where the trajectory first enters the box and the phase space point where the trajectory leaves the box. In fact, this is the average direction of the trajectory through the box during a particular pass. The approximation for the vector field $\mathbf{V}_k$ in the kth box of the phase space is now simply the average vector of all passes obtained according to the equation

$$\mathbf{V}_k = \frac{1}{P_k} \sum_{i=1}^{P_k} \mathbf{e}_i, \tag{4}$$

where P_k is the number of all passes through the kth box. Completing this task for all occupied boxes gives us a *directional* approximation for the vector field of the system. Note that the word directional is stressed since the described method provides no information about how fast the trajectory moves through particular boxes. Therefore, we cannot say anything about the absolute lengths of the obtained vectors. The absolute magnitude of the vector field is, however, not important for the determinism test. What is important is the fact that if the time series originated from a deterministic system, and the coarse grained partitioning is fine enough, the obtained vector field should consist solely of vectors that have unit length (remember that each $\mathbf{e}_i$ is a unit vector). This follows directly from the fact that we demand uniqueness of solutions in the phase space. If solutions in the phase space are to be unique, then the unit vectors inside a particular box must all point in the same direction. In other words, the trajectories inside each box may not cross, since that would violate the uniqueness condition at each crossing. Note that each crossing decreases the size of the average vector $\mathbf{V}_k$. For example, if the crossing of two trajectories inside the kth box occured at right angles,

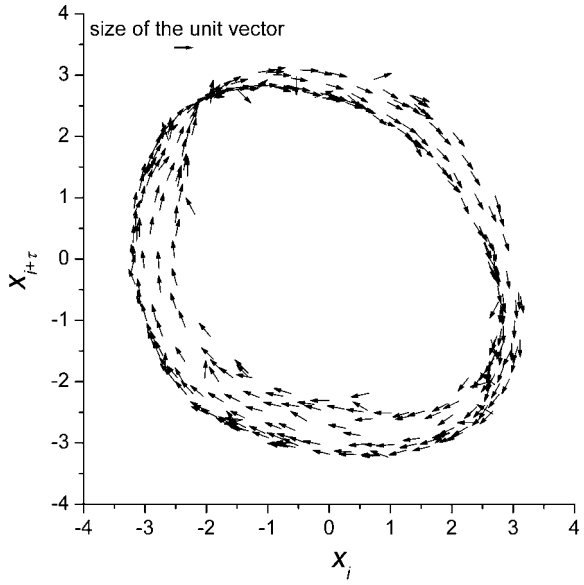

Figure 6. Determinism test. The approximated vector field for the embedding space reconstructed with $\tau = 65$ and $m = 5$. The pertaining determinism factor is $\kappa = 0.83$.

then the size of $\mathbf{V}_k$ would be, according to Pythagoras, $\sqrt{2}/2 \approx 0.707 < 1$. Hence, if the system is deterministic, i.e. no trajectory crossings inside a particular box occur, each average resultant vector obtained according to equation (4) will be exactly of unit length. Accordingly, the average length of all resultant vectors $\mathbf{V}_k$, which we introduce as the definite measure for determinism κ, will be exactly 1, while for a system with a stochastic component this value will be substantially smaller than 1.

The results of the determinism test for the embedding space presented in figure 5 are shown in figure 6. For this calculation the five-dimensional embedding space was coarse grained into a $10 \times 10 \times 10 \times 10 \times 10$ grid. The pertaining determinism factor of the approximated vector field presented in figure 6 is $\kappa = 0.83$. Indeed, it can be well observed that the large majority of vectors are of unit length. However, due to the ever-present measurement error the determinism of the time series is somewhat blurred, consequently yielding $\kappa < 1$. Nevertheless, the deterministic signature is still good enough to be preserved, so that the chaotic appearance of the reconstructed attractor cannot be attributed to stochastic influences. The result presented in figure 6 can be reproduced with the program *determinism.exe*, which can be downloaded from our Web page [20].

3.3. Largest Lyapunov exponent

Lyapunov exponents determine the rate of divergence or convergence of initially nearby trajectories in phase space [25–27]. In general, an m-dimensional system has m different Lyapunov exponents Λ_i, where $i = 1, 2, \ldots, m$. They can be ordered from the largest to the smallest, thereby forming the Lyapunov exponent spectrum $(\Lambda_1, \Lambda_2, \ldots, \Lambda_m)$. Let us consider a three-dimensional system with the Lyapunov exponent spectrum $(\Lambda_1, \Lambda_2, \Lambda_3)$. It has been shown [25–27] that the sign of each Lyapunov exponent uniquely determines the attractor of the system. More precisely, all negative exponents, denoted by $(-, -, -)$, indicate the presence of a fixed point, while $(0, -, -)$ indicates a limit cycle and $(+, 0, -)$ a

chaotic attractor. The most important observation is that the largest Lyapunov exponent Λ_1, denoted as $\Lambda_{\max}$, uniquely determines whether the system is chaotic or not. If $\Lambda_{\max} > 0$, two initially nearby trajectories of the attractor diverge exponentially fast as time progresses, constituting the extreme sensitivity to changes in initial conditions, which is the hallmark of chaos. Thus, for our purposes it suffices to constrain the analysis solely to the largest Lyapunov exponent.

We describe an algorithm developed by Wolf *et al* [28], which implements the theory in a very simple and direct fashion. The first step of the algorithm consists of finding the nearest neighbour of the initial point $\mathbf{p}(0) = (x_0, x_{0+\tau}, x_{0+2\tau}, x_{0+3\tau}, x_{0+4\tau})$. Let L_0 denote the Euclidean distance between them. Next, we have to iterate both points forward for a fixed evolution time t_{evolv}, which should be of the same order of magnitude as the embedding delay τ, and denote the final distance between the evolved points as L_{evolv}. If the attractor is chaotic, L_{evolv} will typically be larger than L_0, whereas in the case of periodicity $L_{\text{evolv}} \approx L_0$. In practice, however, this is true only if t_{evolv} is chosen small enough (usually not larger than $m\tau$) so that the initial length element L_0 is propagated only through the small-scale structure of the attractor. If namely t_{evolv} is too large, it is possible that the two trajectories defining L_0 pass through a folding region of the attractor and thus L_{evolv} will be smaller than L_0, finally leading to an underestimation of the largest Lyapunov exponent ($\Lambda_{\max}$). After each t_{evolv} a replacement step is attempted in which we look for a new point in the embedding space whose distance to the evolved initial point is as small as possible, under the constraint that the angular separation between the evolved and replacement element is small. This procedure is repeated until the initial point $\mathbf{p}(0)$ reaches the end of the time series. Finally, $\Lambda_{\max}$ is calculated according to the equation

$$\Lambda_{\max} = \frac{1}{M t_{\text{evolv}}} \sum_{i=0}^{M} \ln \frac{L_{\text{evolv}}^{(i)}}{L_0^{(i)}}, \tag{5}$$

where M is the total number of replacement steps.

By using equation (5), we calculate the largest Lyapunov exponent for the attractor presented in figure 5. The largest Lyapunov exponent converges very well to $\Lambda_{\max} = 0.33$. This is a firm proof for the chaotic behaviour of the studied experimental system. This final result can be easily reproduced with our program *lyapmax.exe* [20].

4. Discussion

The experimental behaviour of a periodically driven *RLC* circuit was systematically analysed using basic nonlinear time series analysis methods. In particular, we outlined a minimalist, yet careful approach that eliminates the occurrence of so-called false positives, i.e. claims that chaos was found where it was not, but is still simple enough for undergraduate students. Moreover, we developed user-friendly programs for each implemented method [20], which should make the reproduction of presented results possible also for individuals for which this paper represents the first encounter with nonlinear time series analysis.

We applied the mutual information method [17] and the false nearest neighbour method [18] for establishing optimal embedding parameters for the attractor reconstruction from the experimental time series. This enabled us to perform the determinism test [19] and calculate the largest Lyapunov exponent [28]. Thereby, we were able to show that the examined experimental system is deterministically chaotic directly from the time series, without having to construct a mathematical model for the circuit.

The knowledge one obtains when mastering the above-described methods presents a good starting point for performing further nonlinear time series analysis, such as calculation

of dimensions [29–31] or noise reduction [32, 33]. In fact, these tasks would all be appropriate subjects for a sequel paper. Currently, these topics are covered in existing monographs on nonlinear time series analysis [13–15] and in the original papers. An excellent source of information for these methods is also the TISEAN project [34]. Together with the pertaining paper [35] and the book by the same authors [14] the TISEAN project presents a very valuable source of information as well as programs for virtually all topics of nonlinear time series analysis. Therefore, particularly for advanced undergraduate students who would like to delve deeper into nonlinear time series analysis, we recommend exploiting the benefits offered by these sources.

Our goal was to make the methods accessible to undergraduate students, to whom this paper may represent the first contact with the presented theory. The paper is also devoted to teachers who would like to integrate nonlinear time series analysis methods into the physics curriculum.

Appendix. The program package

The whole program package that can be downloaded from our Web page [20] consists of five programs (*embedd.exe*, *mutual.exe*, *fnn.exe*, *determinism.exe* and *lyapmax.exe*) and an input file *ini.dat*, which contains the studied time series. All programs have a graphical interface and display results in the forms of graphs and drawings. In order to run the programs, Windows® environment is required and the input file *ini.dat* has to be in the working directory. After download, the content of the *package.zip* file should be extracted into an arbitrary (preferably empty) directory. Thereafter, the programs are ready to run via double-clicking on the appropriate icon. Initially, a parameter window will appear, which allows you to insert proper parameter values (by default they are set equally to those used in this paper). Once this step is completed, press the OK button to execute the program. A progress bar will appear, which lets you know how fast the program is running, and when it will eventually finish. After completion results are displayed graphically in a maximized window. To avoid exceptionally high memory allocation and running times, all programs are currently limited to operate maximally on 250 000 data points with 10 degrees of freedom. Upon request, we can provide programs that can also handle larger data sets. Finally, we strongly advise the reader to read the manual pertaining to the programs on our Web page [20], where more detailed instructions for users can be found.

References

[1] Lorenz E N 1963 Deterministic nonperiodic flow *J. Atmos. Sci.* **20** 130–41
[2] Rodgers G J 1992 From order into chaos *Phys. Educ.* **27** 14–7
[3] Borcherds P H 1995 The butterfly that stamped: a brief introduction to nonlinear dynamics and chaos *Phys. Educ.* **30** 372–81
[4] Schmidt T and Marhl M 1997 A simple mathematical model of a dripping tab *Eur. J. Phys.* **18** 377–83
[5] Briggs K 1987 Simple experiments in chaotic dynamics *Am. J. Phys.* **55** 1083–9
[6] Nunez Yepez H N, Salas Brito A L, Vargas C A and Vicente L A 1989 Chaos in a dripping faucet *Eur. J. Phys.* **10** 99–105
[7] Hobson P R and Lansbury A N 1996 A simple electronic circuit to demonstrate bifurcation and chaos *Phys. Educ.* **31** 39–43
[8] Martin S J and Ford P J 2001 A simple experimental demonstration of chaos in a driven spherical pendulum *Phys. Educ.* **36** 108–14
[9] Gitterman M 2002 Order and chaos: are they contradictory or complementary? *Eur. J. Phys.* **23** 119–22
[10] MacDonald N and Whitehead R R 1985 Introducing students to nonlinearity: computer experiments with Burgers mappings *Eur. J. Phys.* **6** 143–7
[11] Carretero-Gonzalez R, Nunez-Yepez H N and Salas-Brito A L 1994 Regular and chaotic behaviour in an extensible pendulum *Eur. J. Phys.* **15** 139–48

[12] Barrientos M, Perez A and Ranada A F 1995 Weak chaos in the asymmetric heavy top *Eur. J. Phys.* **16** 106–12
[13] Abarbanel H D I 1996 *Analysis of Observed Chaotic Data* (New York: Springer)
[14] Kantz H and Schreiber T 1997 *Nonlinear Time Series Analysis* (Cambridge: Cambridge University Press)
[15] Sprott J C 2003 *Chaos and Time-Series Analysis* (Oxford: Oxford University Press)
[16] Linsay P S 1981 Period doubling and chaotic behaviour in a driven anharmonic oscillator *Phys. Rev. Lett.* **47** 1349–52
[17] Fraser A M and Swinney H L 1986 Independent coordinates for strange attractors from mutual information *Phys. Rev.* A **33** 1134–40
[18] Kennel M B, Brown R and Abarbanel H D I 1992 Determining embedding dimension for phase space reconstruction using a geometrical construction *Phys. Rev.* A **45** 3403–11
[19] Kaplan D T and Glass L 1992 Direct test for determinism in a time series *Phys. Rev. Lett.* **68** 427–30
[20] http://lizika.pfmb.uni-mb.si/∼matjaz/ejp/time.html (All results presented in this paper can be easily reproduced with our set of programs, which can be downloaded from this Web page.)
[21] Takens F 1981 *Detecting Strange Attractor in Turbulence (Lecture Notes in Mathematics* vol 898) ed D A Rand and L S Young (Berlin: Springer) p 366
[22] Shaw R 1981 Strange attractors, chaotic behavior, and information flow *Z. Naturforsch.* **36a** 80–112
[23] Wayland R, Bromley D, Pickett D and Passamante A 1993 Recognizing determinism in a time series *Phys. Rev. Lett.* **70** 580–2
[24] Salvino L W and Cawley R 1994 Smoothness implies determinism: a method to detect it in time series *Phys. Rev. Lett.* **73** 1091–4
[25] Schuster H G 1989 *Deterministic Chaos* (Weinheim: VCH)
[26] Ott E 1993 *Chaos in Dynamical Systems* (Cambridge: Cambridge University Press)
[27] Strogatz S H 1994 *Nonlinear Dynamics and Chaos* (Reading, MA: Addison-Wesley)
[28] Wolf A, Swift J B, Swinney H L and Vastano J A 1985 Determining Lyapunov exponents from a time series *Physica* D **16** 285–317
[29] Grassberger P and Procaccia I 1983 Characterization of strange attractors *Phys. Rev. Lett.* **50** 346–9
[30] Theiler J 1986 Spurious dimension from correlation algorithms applied to limited time-series data *Phys. Rev.* A **34** 2427–32
[31] Kantz H and Schreiber T 1994 Dimension estimates and physiological data *Chaos* **5** 143–54
[32] Schreiber T 1993 Extremely simple nonlinear noise reduction method *Phys. Rev.* E **47** 2401–4
[33] Grassberger P, Hegger R, Kantz H, Schaffrath C and Schreiber T 1993 On noise reduction methods for chaotic data *Chaos* **3** 127–41
[34] TISEAN project http://www.mpipks-dresden.mpg.de/∼tisean
[35] Hegger R and Kantz H 1999 Practical implementation of nonlinear time series methods: the TISEAN package *Chaos* **9** 413–40